

## EFFECT OF TENSION SOFTENING ON TIME-DEPENDENT DEFORMATION AND CRACK WIDTH OF REINFORCED CONCRETE FLEXURAL MEMBERS

R. Sato, and M. Xu,

Department of Civil Engineering, University of Utsunomiya,  
Utsunomiya, Japan

I. Ujike

Department of Civil & Environmental Engineering, Ehime University,  
Matsuyama, Japan

### Abstract

A numerical analysis method for long-term deformations and crack width in reinforced concrete flexural members under sustained load is proposed based on basic bond equations in consideration of the tensile stress distribution characterized by fictitious crack model at the cracked section. Time-dependent decrease of tension strength and fracture energy of concrete in tension softening curve is assumed in the proposed method. The validity of the present method is verified qualitatively through comparing results obtained by numerical analysis with those by the experiment.

Key words : Reinforced Concrete, Fictitious Crack Model, Flexural Crack Width, Deformation, Bond, Creep, Drying Shrinkage

### 1 Introduction

The application of fracture mechanics to analysis of size effect on concrete structures and so on has been activated, JCI (1993). In the evaluation of deformation and crack width of reinforced concrete (RC) members, tensile stress of concrete at cracked section has generally been neglected not only in design approach but also in numerical analysis approach. However, it is actually observed through experiment that the stress in the reinforcing bar

is smaller than that calculated by the conventional method neglecting tensile stress of the concrete especially in the lower loading level after cracking, Sato et al. (1992a). This means that concrete in tension contributes to resist bending moment at the cracked section. This contribution of concrete in tension should be expected even at the cracked section subjected to sustained bending moment, in the case of concrete members required high performance, for example, controlling crack width less than 0.1 mm at maximum, such as RC members with fibers or expansive agent, or prestressed reinforced concrete member, while tension force in concrete at cracked section will be decreased in RC members, in which tension reinforcement is stressed to the values higher than 100 N/mm<sup>2</sup> at least, as shown later.

Having the above-mentioned situation in mind, in the present research, a numerical analysis method is proposed in order to predict more accurately crack width as well as deformation of RC members under short and long-term loadings, combining the fictitious crack model with analysis method based on bond stress-slip relation formulated for RC flexural members considering the effects of creep and shrinkage, Sato et al. (1992b). Comparison of crack widths and stresses in reinforcing bars obtained from computation with those from experiment is also carried out and the validity of the present analysis method is discussed.

## **2 Analysis procedures**

### **2.1 Basic Assumptions**

In order to derive equations for the analysis of deformation and crack width incorporating fictitious crack model, the following assumptions are made.

- 1) "Plane sections remain plane" holds for the longitudinal strains in concrete compression zone and in concrete tension zone in the vicinity of neutral axis (zone T) and for the strains in compression and tension reinforcing bars.
- 2) The distribution of crack opening displacement (COD) is linear along the depth at cracked section.
- 3) Tensile stress and strain caused by the stress depending on COD at cracked section develop at an arbitrary section between adjacent cracks and the zone length is the same as that at cracked section (zone U).
- 4) The strain in concrete tension at an arbitrary section is distributed superposing strain related to COD in zone U and strain which is proportional to the distance from the stress related neutral axis.
- 5) Drying shrinkage strain is uniform through the section.
- 6) RC element between cracks is symmetrical about the center section.

Based on the above assumptions, the distributions of strain, stress and

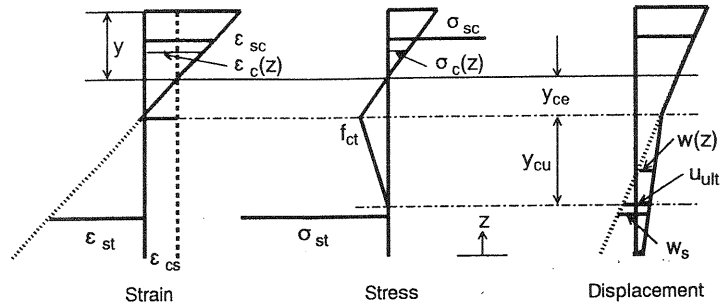


Fig.1 Distributions of strain, stress and crack opening displacement at cracked section

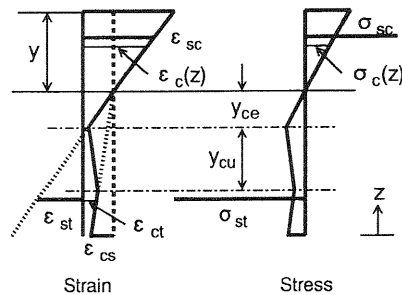


Fig.2 Distributions of strain and stress at an arbitrary section between cracks

displacement at cracked section, and those of strain and stress at an arbitrary section between two adjacent cracks are indicated in Figs.1 and 2.

## 2.2 Basic equations

In order to take the effect of concrete into consideration, effective elastic modulus method is adopted, which is simple and gives good results when concrete stress dose not vary significantly, Neville et al. (1983).

The strain and stress distributions at an arbitrary section with coordinate  $x$  from the center section shown in Fig.2 will be determined if the tensile steel strain  $\epsilon_{st}$ , concrete strain  $\epsilon_{ct}$  at tensile steel position and stress related neutral axis depth  $y$  are given. We have two equations for equilibrium of axial force and bending moment and, therefore,  $\epsilon_{st}$  and  $\epsilon_{ct}$  can be obtained as a function of  $y$ . Differentiation of slip  $s$  with respect to  $x$  is given by the difference between tensile reinforcement strain and concrete strain at the same depth as the steel bar as follows;

$$\frac{ds}{dx} = \frac{\{1+G_{cr}(y)/G_c(y)\} \{M+\Delta M_{sc}(y)+\Delta M_{st}(y)\}}{E_c I_e(y)} (d-y) + \frac{G_{ss}(y)}{G_c(y)} \quad (1)$$

Further differentiating both sides of Eq.(1) with respect to  $x$ , substituting differentiations of  $\epsilon_{st}$  and  $\epsilon_{ct}$  into the equation and replacing  $d\epsilon_{st}/dx=(U_s/A_s E_s)\tau_b(s,x)$ , we obtain the following basic differential equation;

$$\frac{d^2s}{dx^2} = \left[ 1 + \frac{\frac{\partial}{\partial y} \left\{ \frac{G_{cr}(y)}{G_c(y)} \frac{M + \Delta M_{sc}(y) + \Delta M_{st}(y)}{E_e I_e(y)} (d-y) + \frac{G_{ss}(y)}{G_c(y)} \epsilon_{cs} \right\}}{\frac{\partial}{\partial y} \left\{ \frac{M + \Delta M_{sc}(y) + \Delta M_{st}(y)}{E_e I_e(y)} (d-y) \right\}} \right] \frac{U_s}{A_s E_s} \tau_b(s, x) \quad (2)$$

Eq.(2) indicates that bond stress is a function of slip  $s$  and coordinate  $x$  as well as the slip  $s$  and depth of the neutral axis  $y$  are unknown variables. In consideration of that the slip  $s$  is zero at central section and that differentiation of slip ( $=\epsilon_{st}-\epsilon_{ct}$ ) is equal to that calculated at cracked section, the slip  $s$  and depth of neutral axis  $y$  at any section can be obtained by solving Eqs.(1) and (2) simultaneously. Hence by using the solved  $y$  and  $s$ , the concrete strain, steel strain, bond stress and so on will be obtained. The stress at position  $y_{cc}$  which is far from the neutral axis about stress at any section, can be computed simultaneously with distributions of neutral axis depth and curvature in the longitudinal direction.

### 2.3 Cracked section

Based on the assumption 1), the length of zone T from neutral axis to the tip of crack, in which tensile stress develops depending on stress related strain, is obtained as follows;

$$y_{cc} = (f_{ct}/E_c)(d-y)/(\epsilon_{st}-\epsilon_{cs}) \quad (3)$$

as presented in Eq.(3), the stress of tension concrete is determined by steel strain.

The concrete stress in fracture process zone (zone U) can be expressed by Eq.(4) as a function of COD, assuming the linear softening stress-COD relationship;

$$\sigma_{cw}(z) = -(f_{ct}^2/2G_F)w(z)+f_{ct} \quad (4)$$

When the fracture process zone exists within the height of the member, the zone length can be obtained from the following Eq.(5);

$$y_{cu} = (U_{ult}/w_s)(d-y-y_{cc}) \quad (5)$$

Assuming COD at the depth of tension reinforcement, equilibrium of axis force and bending moment gives the depth of neutral axis  $y$  and steel strain by which strain and stress distributions can be obtained.

### 2.4 Analysis procedure

Fig.3 shows the procedure of the present computation, in which crack spacing is given based on observation. As is indicated in the flow, computation is performed iteratively until the steel strain at cracked section obtained from basic bond equations becomes equal to that obtained at cracked section described in 2.3.

The  $y_{cu}$  is calculated by using crack width based on Eq.(5). Analysis is

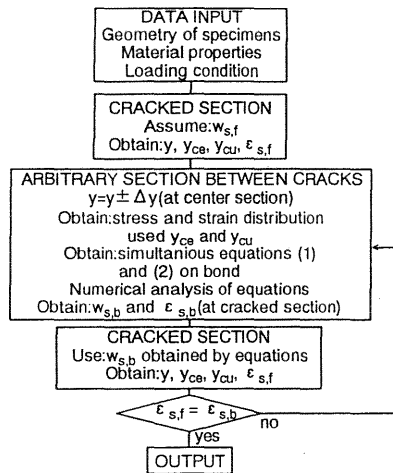


Fig.3 Procedure of numerical analysis

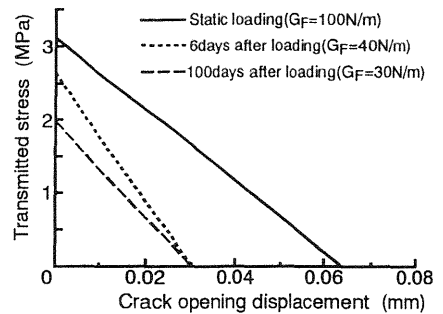


Fig.4 Tension softening diagram

carried out under the condition which the crack propagates above the tensile steel bar.

### 2.5 Softening Stress-COD Curve

Linear softening stress-COD relation shown in Fig.4 is used. The  $f_{ct,i}$  under instantaneous loading is obtained from splitting tensile test. The fracture energy under instantaneous loading  $G_{F,i}$  is assumed to be 100 N/m, JCI (1993). Tensile strength and fracture energy are also assumed to decrease with time as shown in Fig.5, as tensile strength is decreased under sustained high tensile stress, Makizumi et al. (1987).

### 2.6 Model of Bond [Sato et al. (1992b)]

Creep of bond as well as drop of bond strength in the vicinity of crack are considered in bond stress-slip relation which is almost linear under service load condition. Initial bond stiffness is 640 N/mm<sup>3</sup> for steel bar with size

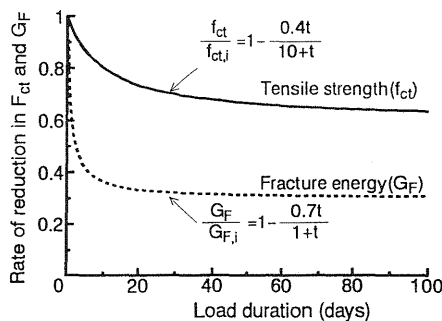


Fig.5 Reduction in tensile strength and fracture energy

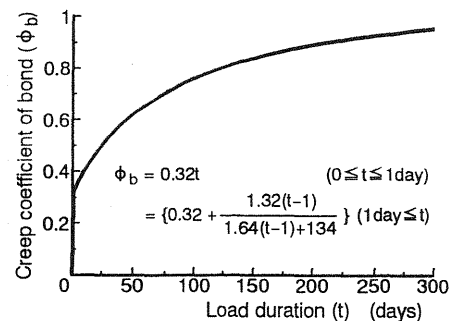


Fig.6 Creep coefficient of bond

of 19 mm. Zone length of drop of bond strength is 1.5D (D : bar diameter) in which bond strength drops linearly toward the crack. Creep coefficient of bond at the time of 350 days after application of load is 0.97, which is defined by ratio of slip at application of instantaneous load to slip increase at the time considered. Creep coefficient of bond adopted in the present computation is shown in Fig.6.

### 3 Experimental procedure

#### 3.1 Specimen

Six reinforced concrete members made in the experiment are 200 mm in width, 250 mm in height and 2400 mm in length as shown in Fig.7. Characteristics of specimens are listed in Table 1. Water cement ratio and unit cement content of concrete are 60% and 290 kg/m<sup>3</sup>, respectively. Creep and drying shrinkage are measured using specimens with the same cross section as RC members. All specimens are cured under wet condition for 33-35 days, then loaded, and exposed to the air in room with constant temperature of 20±1°C and humidity of 60±5%R.H. .

#### 3.2 Loading and measuring

Average curvature, reinforcement strain and crack width are measured in the tested zone with the length of 800 mm subjected to pure bending. Three loads levels corresponding to 100, 150 and 200 N/mm<sup>2</sup> reinforcement stress are applied. The stresses in tension steel of the beams with compression steel are about 15% larger than those of other specimens, because grooved steel bars are arranged. Average curvature is obtained from the deflection measured with dial gauges in the tested zone. In order to measure strain distribution of tension steel deformed bars are grooved and fitted with strain gauges in the zone of 400 mm under pure bending moment. Crack widths are measured with the contact-type strain gauge with a minimum graduation of 1/1000 mm under sustained load. The length of the contact strain gauge between contact points are 20 mm.

Table 1 Outline of specimens

| Specimen | Bar Arrangement | $\rho$ (%) | $\rho'$ (%) | $\sigma_{st}$ (MPa) | $S_r$ (cm) |
|----------|-----------------|------------|-------------|---------------------|------------|
| CS20CR   | ds19*-ds16      | 1.16       | 0.95        | 222                 | 16.6       |
| CS20     | ds19 - 0        | 1.36       | 0           | 197                 | 12.2       |
| CS15CR   | ds19*-ds16      | 1.16       | 0.95        | 167                 | 13.2       |
| CS15     | ds19 - 0        | 1.36       | 0           | 148                 | 14.6       |
| CS10CR   | ds19*-ds16      | 1.16       | 0.95        | 111                 | 14.8       |
| CS10     | ds19 - 0        | 1.36       | 0           | 99                  | 14.2       |

Ds19\*: grooved reinforcing bar,  $\rho = A_s / (bd)$ ,  $\rho' = A_s' / (bd)$

$\sigma_{st}$ : calculated tensile stress at application of load

$S_r$ : average crack spacing observed at application of load

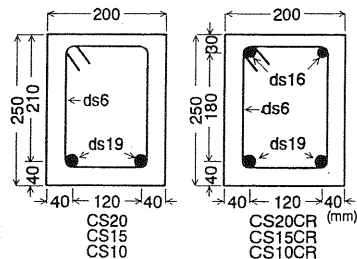


Fig. 7 Details of the cross sections

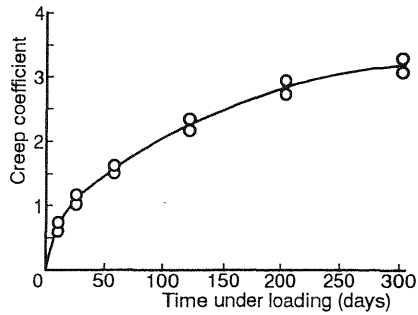


Fig.8 Creep coefficient of concrete

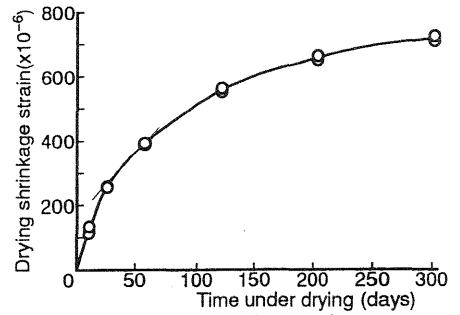


Fig.9 Drying shrinkage of concrete

### 3.3 Properties of materials

Compressive strength, tensile strength and elastic modulus of concrete at the time of loading are  $39.0\text{N/mm}^2$ ,  $3.11\text{N/mm}^2$ ,  $27.5\text{kN/mm}^2$ , respectively. Creep coefficient and drying shrinkage measured are shown in Figs.8 and 9.

### 4 Comparison of analysis and experiment

Typical example of distribution of strain and stress at cracked section as well as that of COD below the tip of crack along the depth obtained by the computation is shown in Fig.10. The present analysis method shows

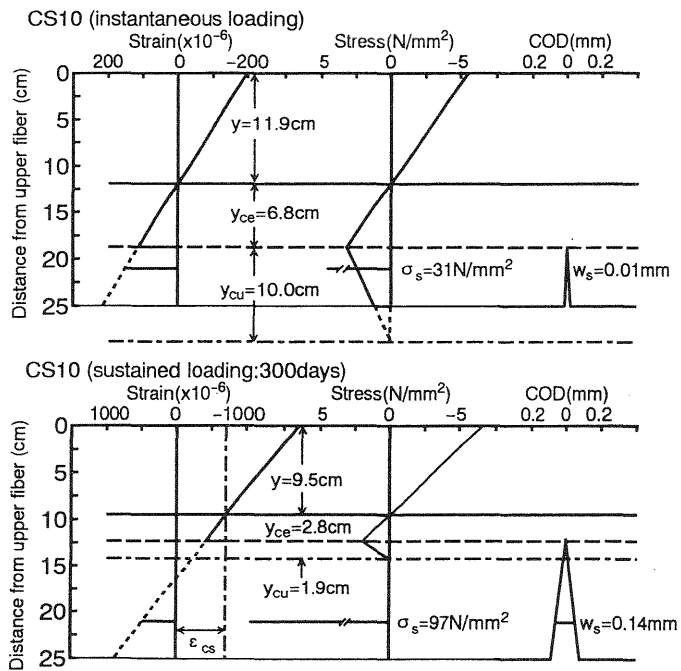


Fig.10 Computed distributions of strain, stress and COD at cracked section

tension reinforcement strain increased with time corresponding to the decrease of fracture process zone, while the companion analysis method neglecting concrete in tension gives less change of the steel strain.

The neutral axis depth changes due to the effect of creep and drying shrinkage of concrete as well as time-dependent decrease of tensile strength and fracture energy. Therefore, tensile stress in a part should be unloaded or reloaded and, however, the effect of unloading and reloading on stress is neglected in the present study, which is not made clear under sustained load.

The effect of tension concrete at cracked section on load-average curvature relationship obtained by the computation is typically shown in Fig.11, compared with that by experimental results. In the analysis stabilized average crack spacing observed at the starting time of application of sustained load is used, though the crack develops in number in the loading stage slightly increased after initial cracking load. The analysis result in consideration of tension softening agrees fairly well with that resulted from experiment, while the change of crack spacing is neglected. On the other hand, the method neglecting concrete tension at

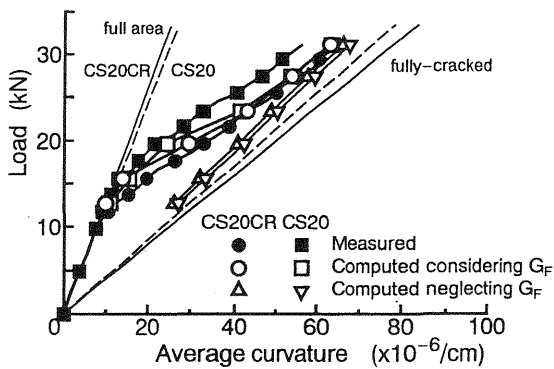


Fig.11 Comparison of measured and computed load-average curvature relationship

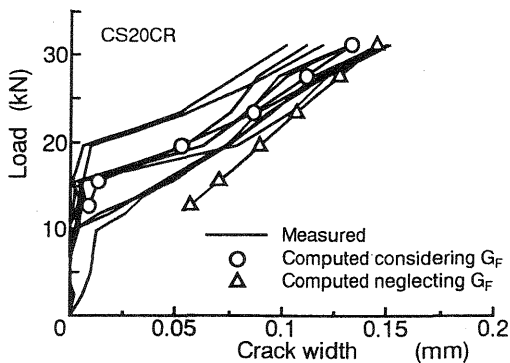


Fig. 12 Comparison of measured and computed load-crack width relationship

cracked section shows constant flexural stiffness and overestimates curvature especially just after initial cracking.

Fig.12 indicates comparison of computed and measured relation between load and crack widths. Crack widths shown in the figure include all crack widths measured on both sides in tested zone. The present analysis considered tension softening predicts crack width with satisfactory accuracy like the case of curvature.

Figs.13 and 14 indicate computed maximum and average tension steel strains varied with time compared with experimentally obtained ones. Measured maximum strain increases rapidly at early time after application of sustained load and then almost becomes constant. It can be seen from the comparison that incorporation the concept of fracture energy depending upon the time into analysis for cracked section improves the accuracy significantly. Increase of reinforcement strain with time contributes to widening of crack with time, Abe et al. (1995) and results in overestimate of the effect of creep and drying shrinkage on time-dependent increase of crack width. As is expressed in Fig.14, the present computation

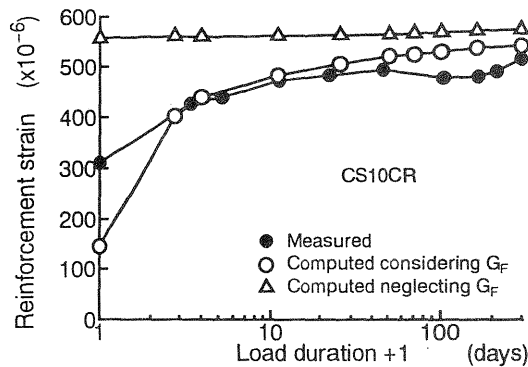


Fig. 13 Comparison of measured and computed time-dependent change of maximum strain in tension reinforcement

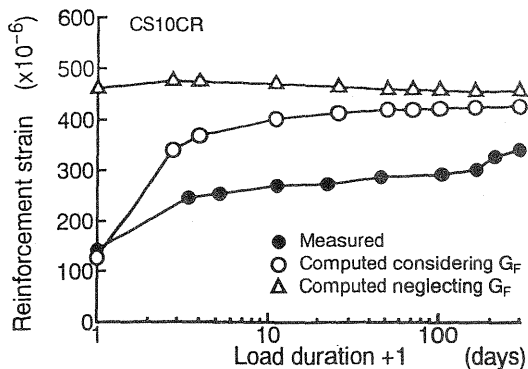


Fig. 14 Comparison of measured and computed time-dependent change of average strain in tension reinforcement

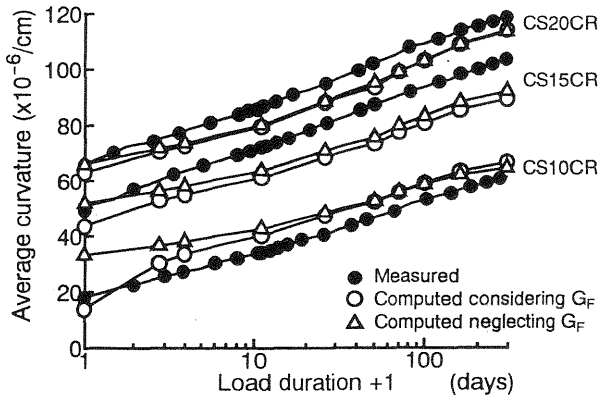


Fig.15 Comparison of measured and computed time-dependent change of average curvature

overestimates average reinforcement strain measured in the specimen. The reason for this could be due to larger decrease of fracture energy with time and/or neglect of crack dispersion and/or neglect of new development of invisible cracking in tension concrete between adjacent cracks.

Comparisons of average curvature-load duration relationships obtained by the computation and those by experiment are shown in Fig.15. As is shown in the figure, rapid increase at early stage after loading is also observed in curvature which is not so predominant as reinforcement strain, because curvature is influenced by strain in compression concrete. The reason of curvature underestimated by the present analysis for members arranged with reinforcing bar in compression is the use of effective elastic modulus method for modeling creep of concrete.

Figs.16 and 17 shows comparison of crack widths computed considering tension softening and those ignoring that for various ages. Tension stresses in reinforcing bars of the beams are 200 and 150 N/mm<sup>2</sup>,

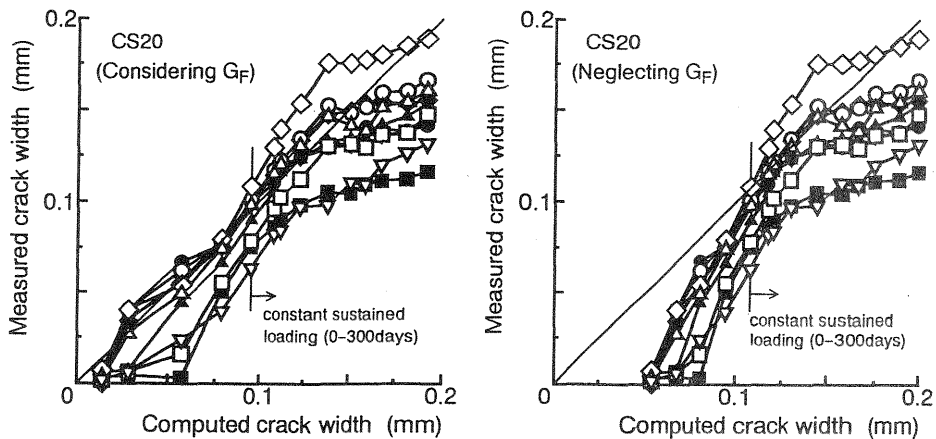


Fig.16 Comparison of measured and computed crack width

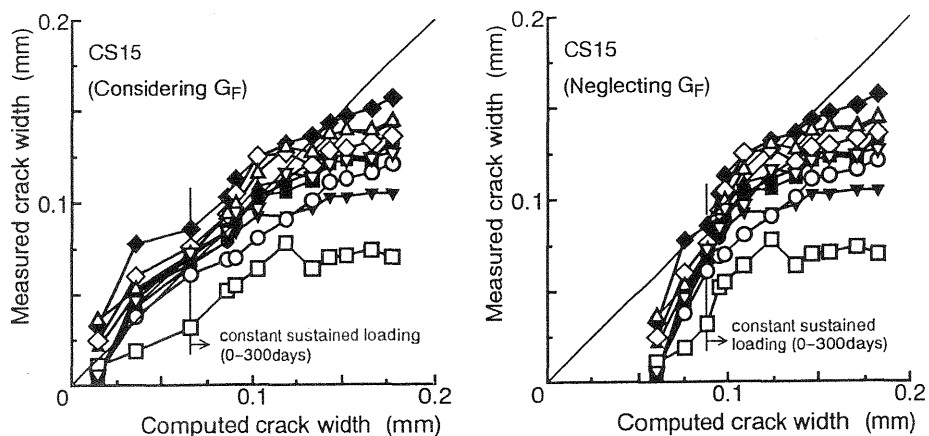


Fig. 17 Comparison of measured and computed crack width

respectively. As shown in both figure, considering tension softening, the accuracy of prediction is significantly improved for crack width smaller than 0.1 mm. However, long-term crack widths for both beams are overestimated irrespective of presence and absence of consideration of fracture energy. This must be explained by the fact that stiffness of tension concrete decreases apparently due to development of microcracks, which are produced by remarkable reinforcement restraint for drying shrinkage induced deformation of tension concrete when drying shrinkage strain exceeds  $300 \times 10^{-6}$ , which is not considered in the present analysis, Sato et al. (1995).

## 5 Conclusion

A numerical analysis method for time-dependent deformation and crack width is presented, combining tension softening effect in concrete at cracked section with basic bond equation already developed for reinforced flexural element between adjacent two cracks subjected to sustained load. The feature of the present method exists in dealing systematically with creep and drying shrinkage of concrete, bond stress-slip relation and its creep effect, tension softening and its creep effect, in which crack opening displacement is obtained computationally. The present method improves the analysis results in terms of accuracy concerning with curvature, reinforcement strain and crack width under instantaneous load as well as with those in early period after application of sustained load. The present method would be effective in estimating time-dependent deformation and crack width of concrete members expected performance of high quality which is required to control strictly crack width less than a smaller value, improving model for tension softening and the effect of microcracking in tension concrete between cracks under sustained load.

## 6 References

- Abe, T., Sato, R., Ujike, I. And Tottori, S. (1995) On long-term flexural crack widths of reinforced concrete members subjected to alternating drying and wetting, **Proceedings of the Japan Concrete Institute**, 17(2), 1025-1030.
- JCI (1993) **Application of fracture mechanics to concrete structures**, Technical Committee Report.
- Makizumi, T. and Ohta, T. (1987) Shrinkage cracking of concrete subject to the external uniaxial restraint, **Proceedings of the Japan Society of Civil Engineers**, 378(6), 137-146
- Neville, A.M., Dilger, W.H. and Brooks, J.J. (1983) **Creep of plain & structural concrete**, Construction Press.
- Sato, R., Ujike, I., Minato, H. and Hojyo, Y. (1992a) Studies on long-term deformation and bond in reinforced concrete flexural members, **Proceedings of the Japan Concrete Institute**, 14(2), 63-65.
- Sato, R., Ujike, I., Minato, H. and Dilger, W.H. (1992b) Basic bond equations in a reinforced concrete flexural element, **Proceedings of International Conference on Bond in Concrete**, 1, 2-89-2-98.
- Sato, R., Ujike, I. and Tottori, S. (1995) Long-term flexural crack widths at different ambient conditions, **Building for the 21st Century**, 3, 1973-1978

## Notation

|                        |  |
|------------------------|--|
| $M$                    | = applied sustained bending moment   |
| $\Delta M_{sc}(y)$     | = $\{y_{ct}-(d'-y)\}A_sE_sE_{cs}$  |
| $\Delta M_{st}(y)$     | = $\{y_{ct}-(d-y)\}A_sE_sE_{cs}$   |
| $d, d'$                | = distance from extreme compressive fiber to tensile and compressive reinforcing bar |
| $E_{cs}$               | = drying shrinkage strain  |
| $I_e(y)$               | = $I_{cr}(y)-G_{cr}(y)y_{ct}$ , $y_{ct} = I_c(y)/G_c(y)$                             |
| $I_{cr}(y), G_{cr}(y)$ | = $I_c'(y)+n_e I_s'(y)+n_e I_s(y)$ , $G_c'(y)+n_e G_s'(y)+n_e G_s(y)$                |
| $I_c'(y), I_s'(y)$     | = second moments of area of concrete and steel in compression zone about the N.A.    |
| $I_c(y), I_s(y)$       | = second moments of area of concrete and steel in tension zone about the N.A.        |
| $G_c'(y), G_s'(y)$     | = first moments of area of concrete and steel in compression zone about the N.A.     |
| $G_c(y), G_s(y)$       | = first moments of area of concrete and steel in tension zone about the N.A.         |
| $A_s', A_s$            | = areas of reinforcements in compression and tension zone                            |
| $E_s, E_c(t_0)$        | = elastic modulus of reinforcement and concrete at the age $t_0$                     |
| $E_e, n_e$             | = $E_c(t_0)/\{1+\phi(t, t_0)\}$ , $E_s/E_e$  |
| $\phi(t, t_0)$         | = creep coefficient of concrete at age $t$ for loading at age $t_0$                  |
| $t, t_0$               | = ages of concrete when the strain is considered and when the load is applied        |
| $G_{ss}(y)$            | = $n_e(A_s'+A_s)(d-y)$   |
| $\tau_b(s, x), U_s$    | = bond stress, perimeter of tension reinforcement                                    |
| $f_{ct}$               | = tensile strength of concrete   |
| $w(z)$                 | = $(h-z-y_{ce})w_s/(d-y_{ce})$ , $h$ = height of member                              |
| $w_s$                  | = crack opening displacement at the depth of tension reinforcement                   |
| $G_F$                  | = fracture energy  |
| $U_{ult}$              | = $2G_F/f_{ct}$  |